Life Sciences 237 (2019) 116945

Contents lists available at ScienceDirect

Life Sciences

journal homepage: www.elsevier.com/locate/lifescie

MiR-216b-5p inhibits cell proliferation in human breast cancer by down-regulating HDAC8 expression

Mohammad-Nazir Menbari[a], Karim Rahimi[b,c], Abbas Ahmadi[d], Anvar Elyasi[e], Nikoo Darvishi[a], Vahedeh Hosseini[d], Samira Mohammadi-Yeganeh[f,g,**], Mohammad Abdi[a,h,*]

[a] Cellular and Molecular Research Center, Research Institute for Health Development, Kurdistan University of Medical Sciences, Sanandaj, Iran
[b] Department of Molecular Biology and Genetics, Gene Expression and Gene Medicine, Aarhus University, Aarhus, Denmark
[c] Interdisciplinary Nanoscience Center, Aarhus University, Aarhus, Denmark
[d] Department of Molecular Medicine and Genetics, Faculty of Medicine, KurdistanUniversity of Medical Sciences, Sanandaj, Iran
[e] Department of Surgery, Faculty of Medicine, Kurdistan University of Medical Sciences, Sanandaj, Iran
[f] Medical Nanotechnology Research Center, Shahid Beheshti University of Medical Sciences, Tehran, Iran
[g] Department of Biotechnology, School of Advanced Technologies in Medicine, Shahid Beheshti University of Medical Sciences, Tehran, Iran
[h] Department of Clinical Biochemistry, Faculty of Medicine, Kurdistan University of Medical Sciences, Sanandaj, Iran

ARTICLE INFO

Keywords:
Breast cancer
Cancer progression
HDAC8
miR-216b-5p

ABSTRACT

Aim: Over-expression of histone deacetylase 8 (HDAC8) has been demonstrated in breast cancer. But the underlying molecular mechanism of HDAC8 on the progression of breast cancer remains unknown. MicroRNAs (miRs) are proposed as important molecules in cancer progression by targeting specific oncogenes or tumor-suppressor genes. Our overall objective was to assess the miR-216b-5p role on HDAC8; and its impacts on breast cancer (BC) progression.

Main methods: We acquired cancerous and noncancerous tissues from Iran Tumor Bank (I.T.B). The MDA-MB-231, MCF-7 and MCF-10A BC cell lines were also purchased. The tissue and cell line expression levels of miR-216b-5p and HDAC8 were determined by quantitative real-time PCR (qPCR). We next measured protein levels of HDAC8 by Western blotting assay. The cell cycle, cell proliferation, and colony formation assay were determined. Finally, we investigated the role of HDAC8 using a knockout vector; and confirmed the targeting of 3′ untranslated region (3′-UTR) of HDAC8 through miR-216b-5p using a luciferase reporter assay.

Key findings: Our results demonstrated a significant decrease in miR-216b-5p, and remarkable increase in HDAC8 levels within human breast cancer tissues and cell lines. The lower levels of miR-216b-5p were negatively correlated with lymph node metastasis and advanced tumor size. The overexpression of miR-216b-5p in BC cell lines inhibited cellular proliferation and progression. HDAC8 was directly down-regulated by miR-216b-5p and knockout of HDAC8 showed the similar effects as miR-216b-5p overexpression.

Significance: Briefly, HDAC8 is an oncogene that accelerate breast cancer proliferation and progression and miR-216b-5p modulates those functions by binding to HDAC8 3′-UTR.

1. Introduction

Breast cancer (BC) is known as the most prevalent malignancy in women worldwide, which accounts for 26% of all cancers by 182,000 new cases, annually [1]. BC is a complicated and complex disease characterized by the growth of malignant cells in the mammary glands with a great number of aberrations at the pathologic, genomics, epigenetics, and molecular level which eventually result in the dysregulation of gene expression and signaling pathways [2].

Aberrant expression of histone deacetylases (HDACs) are related to tumor pathogenesis, progression, and prognosis [3]. Therefore, these enzymes are among the most potential biomarkers and therapeutic targets for cancer detection and treatment [3]. Recently, HDAC inhibitors have gotten more attention as potential therapeutic agents for treatment of some malignancies [3,4]. Among them, HDAC8 is the most recently identified class I HDACs which is linked to a number of

* Corresponding author. Department of Clinical Biochemistry (room No. 384), Faculty of Medicine, Kurdistan University of Medical Sciences, Pasdaran Boulevard, Postal code: 6618634683, Sanandaj, Iran.
** Corresponding author. Medical Nanotechnology Research Center, Shahid Beheshti University of Medical Sciences, Tehran, Iran.
E-mail addresses: s.mohammadiyeganeh@sbmu.ac.ir (S. Mohammadi-Yeganeh), abdi@muk.ac.ir (M. Abdi).

https://doi.org/10.1016/j.lfs.2019.116945
Received 17 August 2019; Received in revised form 22 September 2019; Accepted 7 October 2019
Available online 09 October 2019
0024-3205/

diseases particularly to hematological malignancies [5]. Recent studies showed that HDAC8 is a potential Oncogene; and its high expression is directly related to several malignancies [4,6–8]. HDAC8 inhibition showed anti-tumor activity and increased the apoptotic cells ratio in T cell lymphomas [9]. Furthermore, it seems that HDAC8 involves in the pathogenesis of neuroblastoma [8]. It has been recently demonstrated that HDAC8 is up-regulated in BC cells and proposed this molecule as a potential oncogene in breast cancer [6].

MicroRNAs (miRs) are natural RNA molecules that play critical roles in cellular processes and regulate gene expression post-transcriptionally. MiRs are known as a type of small non-coding RNAs with 19–25 bp length that are cleaved from a 70–100 bp hairpin pre-miRNA precursors [10]. Single-stranded mature miR binds to the 3′ untranslated region (3′-UTR) of the target mRNA and regulated the block of translation or degradation of targeted mRNA molecule [10]. According to the literature, the aberrant expression of numerous miRs is associated with various human malignancies [11]. Among them, miR-216b-5p is a newly recognized miR that acts as a tumor suppressor. In nasopharyngeal carcinoma, researchers suggested that the anti-tumor effects of miR-216 applies via PKC and KRAS [12,13]; miR-216 is also inhibit proliferation of BC cells possibly by targeting syndecan binding protein (SDCBP) [14] and P2X7 receptor (P2X7R) [15].

The concurrent association between miR-216 and HDAC8 with progression of breast cancer is not understood yet. Also, to the best of our knowledge, there is no other study in evaluating the miR-216 and HDAC8 role in the carcinogenesis of breast cancer. Hence, in the this study we aimed to study the miR-216b-5p and HDAC8 levels in cancerous and adjacent none-cancerous tissues obtained from BC patients; and the specific objective was to assess the potential role of HDAC8 and miR-216 (as a potential inhibitor of the HDAC8) on tumor growth in human breast adenocarcinoma.

2. Material and methods

2.1. Patients and tissue collection

We obtained 32 tissue specimens from Iran Tumor Bank (I.T.B) during the period January 2016-January 2018. We then obtained control samples from normal adjacent tissue; and subsequently, we confirmed both the malignant and normal tissues, pathologically. We then obtained the written informed consent from all studied subjects. In this case, we got the approval from ethics committee of Kurdistan University of Medical Sciences. We then excluded those patients with a history of other organ cancers from the employed dataset in this study. We also used the Scarf–Bloom–Richardson criteria and the TNM staging system for breast cancer in tumor grading and evaluating the clinical staging of patients, respectively [16,17]. We finally obtained the information on morphologic characteristics, grade, and stage of the tumor from the medical records (see Table 1 for details).

2.2. Cell lines and cell culture conditions

Human Embryonic Kidney 293T (HEK293T) cell line and BC cell lines including MCF-7 and MDA-MB-231 and also an immortalized normal breast epithelial cell line, MCF-10A as control, were purchased from the International Centre for Genetic Engineering and Biotechnology (ICGEB) (Tehran, Iran). Upon collecting the dataset, we seeded the MCF-7, MDA-MB-231 and HEK293T cell lines in RPMI-1640 medium supplemented with 10% fetal bovine serum (FBS). Then we cultured the MCF-10A cell line in DMEM:Ham's F12 (1:1) supplemented with 5% Horse serum, 2 mmol L-Glutamine, 10 μg/ml Insulin, 20 ng/ml Epithelial growth factor (EGF), 0.5 μg/ml Hydrocortisone and 100 ng/ml cholera toxin. All cells were incubated at 37 °C in a humidified 5% CO_2 atmosphere.

2.3. In-Silico prediction of miRs

In regard to *In-Silico* prediction of miRs, we obtained the HDAC8 gene sequence from NCBI database (i.e., NG_015851.1). To predict the miRs that target the 3′-UTR of HDAC8 with the highest possibility, we employed the following databases: Diana-microT, RNA22, TargetScan, PicTar, miRanda, miRDB, and mirPath. Then, we applied mirZ database to identify miR targets in comparison to their expression in different cell lines and miRCancer, Qiagen and dbDEMC 2.0 databases in order to provide a miRs list in various human cancers. Finally, we utilized the miRnalyze and DIANA-miRPath v3.0 databases to determine the role of the predicted/modelled miRs in HDAC8 signaling pathways (Table 2).

2.4. RNA purification and quantitative real-time PCR (qRT-PCR) analysis

According to the manufacturer's instruction, we first extracted the total RNA containing small RNAs from cancerous, normal tissues and cell lines using RNX™-Plus reagent (Cinnagen, Tehran, Iran). Then, we synthesized the cDNA from total RNA using RevertAid First Strand cDNA Synthesis Kit (Fermentas – Thermo Scientific) according to the manual. Then, we performed the quantitative real-time PCR with a SYBR Premix ExTaqII kit (Takara, Japan) and the Rotor-Gene 6000 apparatus (Corbett Research, Mortlake, NSW, Australia). MiRs expression was quantified using an SYBR^R Premix ExTaq™ kit (Takara, Japan) according to the manufacturer's instruction. *HPRT* and *SNORD47 (U47)* were employed for mRNA and miR data normalization, respectively. Primers used for qPCR and construction of using vectors are listed in Table 3.

2.5. CRISPR/Cas9 mediated knockout of the HDAC8 gene in MCF-7 and MDA-MB-231 cell line

The expression of *HDAC8* in the MCF-7 and MDA-MB-231 cell lines were knocked out (KO) by applying the CRISPR/Cas9 based KO strategy. Then, we designed the CRISPR sgRNAs using crispr.mit.edu and ordered the oligos for synthesis to Macrogen Inc. (Seoul, Korea). pCAG-eCas9-GFP-U6-gRNA vector (Addgene 79145) without ITR element [18] was digested with BbsI enzyme for gRNA cloning. The gRNAs sequences used in knocking out the *HDAC8* gene are illustrated in Table 3. The prepared eCas9/gRNA expression vectors co-transfected to the cell lines using Lipofectamine 2000, according to the manufacture instruction (Invitrogen, Carlsbad, CA, USA). Finally, we used the eCas9 expression vector without any cloned gRNA for the control.

2.6. Transient transfection

We cultured MCF-7 and MDA-MB-231 cell lines in six-well plates at a density of 1.5×10^5 cells/well and grown to 90% confluency. Then, the cells were transiently transfected with 100 nM miR-216b-5p mimics, negative control and inhibitor (Exiqon). We next performed transfection by Lipofectamine 2000 according to the manufacturer's instructions. After transfection, we kept cells in a culture medium containing 10% FBS for up to 72 h. Finally, we extracted total RNA and protein and used for further investigations.

2.7. Luciferase reporter assay

In this phase, the PCR purified HDAC8 3′-UTR (WT-UTR) sequence containing the predicted miR-216b-5p binding sites was cloned into the psiCHECK™-2 Vector (Promega, Madison, USA) using specific primers for HDAC8 3′-UTR (Table 3). We digested the vector using SgfI and NotI restriction enzymes. A mutant luciferase vector with miR-216b-5p changed pairing site (Mut-UTR) was also constructed. Wild and mutant types of HDAC8-UTR plasmid were confirmed by DNA sequencing. When HEK293T cells reached 80% confluence in 24-well plate, cells were co-transfected with luciferase vector and miR-216b-5p mimic,

Table 1
Clinical characteristics of studied subjects.

Sample	site	Type of breast cancer	Stage of disease	Expression of hormone receptors			Necrosis	Invasion to other tissues		
				ER	PR	Her2/neu		Lymphatic invasion	Vascular invasion	perineural invasion
1	Right breast	infiltrating ductal carcinoma	III	Neg	Neg	Neg	Yes	Yes	Yes	No
2	Right breast	invasive ductal carcinoma	III	Neg	Neg	Neg	Yes	Yes	No	No
3	Left breast		III	Neg	Neg	Neg	Yes	Yes	Yes	
4	Right breast	invasive lobular carcinoma	I	Neg	Neg	Neg	No	Yes	No	Yes
5	Left breast		III	Neg	Neg	Neg	Yes	Yes	Yes	
6	Right breast	invasive ductal carcinoma	II	Neg	Neg	Neg	No	No	No	No
7	Left breast	invasive ductal carcinoma	II	Neg	Neg	Neg	Yes	Yes	Yes	No
8	Left breast	invasive ductal carcinoma	III	Neg	Neg	Neg	Yes	Yes	Yes	
9	Left breast	Fibroadenoma	III	Neg	Neg	Neg	Yes	Yes	Yes	
10	Left breast	invasive ductal carcinoma	II	Neg	Neg	Neg	No	Yes	No	No
11	Right breast	–	III	Neg	–	Neg	Yes	Yes	Yes	Yes
12	Left breast	invasive ductal carcinoma	III	Neg	Neg	Neg	Yes	Yes	No	No
13	Right breast	invasive ductal carcinoma	III	Neg	Neg	Neg	Yes	Yes	No	No
14	Left breast	Infiltrating ductal	III	Neg	Neg	Neg	No	Yes	Yes	No
15	Left breast	invasive ductal carcinoma	I	–	–	–	–	Yes	Yes	Yes
16	Left breast	invasive ductal carcinoma	I	–	–	–	–	No	No	No
17	Left breast	Inflammatory mammaty	III	Neg	Neg	Neg	–	No	No	Yes
18	Left breast	Infiltrating ductal	III	Neg	Neg	Neg	Yes	No	No	No
19	Right breast	Infiltrating ductal	III	Neg	Neg	Neg	Yes	No	No	No
20	Right breast	invasive ductal carcinoma	III	Neg	Neg	Neg	No	Yes	Yes	Yes
21	Left breast	Infiltrating ductal	III	Neg	Neg	Neg	Yes	Yes	Yes	No
22	Left breast	Infiltrating ductal	I	Neg	Neg	Neg	Yes	Yes	Yes	No
23	Right breast	invasive ductal carcinoma	II	Neg	Neg	Neg	No	Yes	Yes	No
24	Right breast	invasive ductal carcinoma	IV	–	–	–	Yes	Yes	Yes	Yes
25	Right breast	invasive ductal carcinoma	III	Neg	Neg	Neg	Yes	Yes	No	No
26	Right breast	invasive ductal carcinoma	III	Neg	Neg	Neg	Yes	Yes	Yes	No
27	Right breast	Infiltrating ductal	III	Neg	Neg	Neg	Yes	Yes	No	No
28	Left breast	invasive ductal carcinoma	II	Neg	Neg	Neg	Yes	Yes	Yes	Yes
29	Left breast	invasive ductal carcinoma	III	Neg	Neg	Neg	Yes	Yes	–	Yes
30	Right breast	Infiltrating ductal	II	Neg	Neg	Neg	No	Yes	–	–
31	Left breast	invasive ductal carcinoma	II	Neg	Neg	Neg	No	No	–	–
32	Left breast	invasive ductal carcinoma	I	Neg	Neg	Neg	No	No	–	–

ER: Estrogen receptor; PR: Progesterone receptor; Her2/neu: human epidermal growth factor receptor 2.

Table 2
Databases and algorithms for determination of target mRNAs and corresponding miRs.

Database	Algorithm	Website
miRanda	Complementarity	http://www.kcc.org
TargetScan	Seed complementarity	http://www.targetscan.org
TargetScanS	Seed complementarity	http://www.targetscan.org
DIANA microT	Thermodynamics	http://diana.pcbi.upenn.edu
PicTar	Thermodynamics	http://pictar.bio.nyu.edu
RNAHybrid	Thermodynamics	http://bibiserv.techfak.unibielefeld.de/rnahybrid
miTarget	SVMe	http://cbit.snu.ac.kr/~miTarget
miTarget	validated targets	http://diana.pcbi.upenn.edu/tarbase.html
miRwalk	Integrative	http://www.ma.uni-heidelberg

Table 3
Primers used for qPCR and construction of using vectors.

Primer	Sequence	TM	Product size
HPRT1-Forward	CCTGGCGTCGTGATTAGTG	58	125
HPRT1-Reverse	TCAGTCCTGTCCATAATTAGCC		
HDAC8-Forward	GGCTGCGGAACGGTTTTAAG	58	166
HDAC8-Reverse	GCTTCAATCAAAGAATGCACCATAC		
HDAC8-gRNA 1+	CCGGCGATCTCAAGAATAGG	–	–
HDAC8-gRNA 1-	CCTATTCTTGAGATCGCCGG	–	–
HDAC8-gRNA 2+	CAGTCACCAGTTTGTAGGGC	–	–
HDAC8-gRNA 2-	GCCCTACAAACTGGTGACTG	–	–
HDAC8 3′-UTR-F	CATTTGCATAGCCTTGTCTG	54	898
HDAC8 3′-UTR-R	GAGTGTTAATCTTCCCAAGCA	54	

inhibitor and negative control using Lipofectamine 2000. Then we measured the luciferase activities after 48 h using a dual-luciferase reporter assay system (Promega, Madison, US) according to the manufacturer's instructions.

2.8. Cell cycle analysis

Flow cytometry was applied for cell cycle assessment in different groups. Briefly, 72 h after transfection, cells were collected and fixed with 70% ethanol at 1 h at 4 °C. The fixed cells washed with PBS, then incubated with propidium iodide (PI) (Sigma-Aldrich) at room temperature for 1 h and samples were analyzed using a BD FACScalibur flow cytometer (BD Biosciences, Mountain View, CA).

2.9. Cell proliferation assay

We cultured MCF-7 and MDA-MB-231 cell lines in a 96-well plate at 5000 cells per well then the cells were transfected with miR-216b-5p mimic, negative control and inhibitor and incubated for six consecutive days. We assessed cell viability after transfection using a commercial 3–2, 5-diphenyl tetrazolium bromide (MTT) assay kit (Sigma, St Louis, MO) according to the manufacturer's instructions at designated times (6 consecutive days). Finally, we measured the absorbance of each well at 450 nM.

2.10. Colony formation assay

Firstly, the MCF-7 and MDA-MB-231 cell lines were transfected with miR-216b-5p mimic, negative control, inhibitor and HDAC8 knockout vector in 6-well culture dishes. The plates were covered with a layer of 0.6% agar in a medium supplemented with 20% FBS. A total of 1000 cells were prepared in 0.3% agar and incubated for 14 days at 37 °C and 5% CO2 conditions. The resulting colonies stained with 0.04% crystal violet for 40 min, then rinsed with PBS again. Finally, the numbers of colonies per well were counted.

2.11. Western blotting

We lysed all samples by a RIPA buffer containing protease and phosphatase inhibitor cocktail and incubated for 10 min at 4 °C. Then, protein concentration was measured using the bicinchoninic acid (BCA) protein assay kit (Bio basic, Canada). After electrophoresis of 40 μg of the lysates in 12% SDS-PAGE, the gel transferred on a PVDF membrane (Millipore, USA). The membrane were blocked by Non-fat milk powder (5%) and subsequently incubated overnight with primary antibodies (Santa Cruz, 10513). At the next day, all samples were incubated with HRP-labeled secondary antibodies (Minneapolis, MN 55413). Finally, the signals were detected using an ECL detection kit (Sigma-Aldrich), and the membranes were scanned and analyzed using ImageJ 1.34I software (NIH).

2.12. Statistical analysis

SPSS 16 (SPSS Inc., Chicago, USA) was used for statistical analyses. Results were presented as Mean ± SD of three independent experiments and comparison of the possible differences between studied groups were done by the independent samples T test. One Way ANOVA followed by Post Hoc, Tukey, and Dunnett tests were used to analyze mean differences between more than two groups. The association between two variables was calculated using the Spearman correlation coefficient. In all performed hypothesis tests, a P value less than 0.05 was considered as statistically significant.

3. Results

3.1. Expression of HDAC8 and miR-216b-5p in breast cancer cell lines and clinical specimens

In analyzing the clinicopathologic status, we detected the expression of HDAC8 and miR-216b-5p in 32 primary breast cancer tissues and 32 normal adjacent tissues using qRT-PCR. The expression of miR-216b-5p in cancerous tissues were significantly decreased in compared with normal adjacent tissues (0.0024 ± 0.00025 (r.u.) *vs.* 0.004 ± 0.00044 (r.u.), respectively) (Fig. 1A and B) (p value = 0.002). Our results also revealed that miR-216b-5p expression is decreased in metastatic breast cancer cell line MDA-MB-231 compared to non-metastatic (MCF-7) and control (MCF-10A) cell lines (0.00095 ± 0.00001 (r.u.), 0.0048 ± 0.00008 (r.u.) and 0.0062 ± 0.0001 (r.u.), respectively) (Fig. 1C). On the other hand, we found that HDAC8 expression level was highly increased in breast cancer tissue samples than normal adjacent tissues (4.86 ± 0.44 (r.u.) *vs.* 3.52 ± 0.43 (r.u.), respectively) (Fig. 1D and E) (p value = 0.034). Additionally, our results showed that the HDAC8 was also up-regulated in breast cancer (MDA-MB-231 and MCF-7) cell lines as compared to control (MCF-10A) cell line (0.32 ± 0.0092 (r.u.), 0.29 ± 0.01 (r.u.) and 0.1 ± 0.0097 (r.u.), respectively) (Fig. 1F). Finally, linear regression analysis confirmed that there was a negative significant correlation statistically between HDAC8 and miR-216b-5p in clinical specimens and cell lines (r^2 = 0.3952, p value = 0.037, Fig. 1G).

Besides, our results showed that the decreased level of miR-216b-5p was significantly associated with tumor size and lymph node invasion (Spearman's ρ = -0.382, p value = 0.041 and Spearman's ρ = -0.373, p value = 0.039). There was not any significant association between HDAC8 tissue level and clinical outcomes (Table 4).

3.2. Effects of ectopic expression of miR-216b-5p on cell proliferation, cell cycle, and colony formation

To study the role of miR-216b-5p in BC cells, MCF-7 and MDA-MB-231 cell lines were transiently transfected with miR-216b-5p mimics

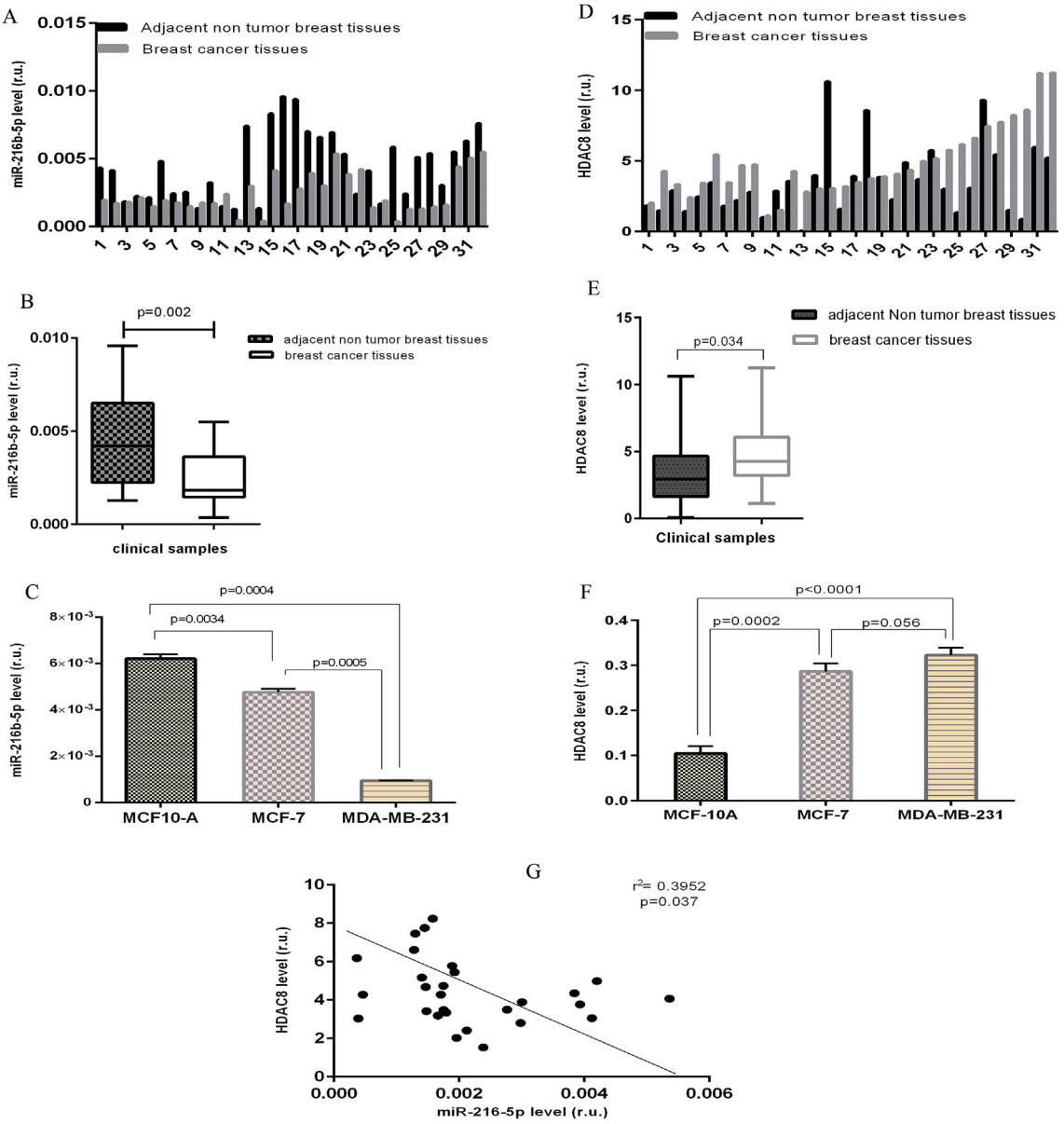

Fig. 1. Relative expression level of miR-216b-5p and HDAC8 in breast cancer tissues and matched normal adjacent cancer tissues: 1A: miR-216b-5p level (in r.u.) separately illustrated in studied subjects 1B: miR-216b-5p level (in r.u.) are indicated as a gray value was in a lower concentration 2.4 ± 0.25 (× 10^{-3}r.u.) for the cancer group and increasing concentration to 4 ± 0.44 (× 10^{-3}r.u.) for normal tissues with a significant *p* value = 0.002 for their difference. 1C: miR-216b-5p levels (in relative units) are indicated as a column value of 100% for the MCF-10A control cell line and decreasing percentage to 77% (0.23 fold decrease) for non-metastatic MCF-7 cell line and lower to 15.32% (0.85 fold decrease) for the metastatic MBA-MD-231 cell line with a lower significant *p* value of 0.0004 for their difference. 1D: HDAC8 level (in r.u.) separately illustrated in studied subjects. 1E: HDAC8 level (in r.u.) are indicated as a gray value was in a higher concentration (4.86 ± 0.44 (r.u.)) for the cancer group and decreasing concentration to 3.52 ± 0.43 (r.u.) for normal tissues with a significant *p* value = 0.034 for their difference. 1F: HDAC8 levels (in relative units) are indicated as a column value of 100% for the MCF-10A control cell line and increasing percentage to 290% (0.29 fold increase) for non-metastatic MCF-7 cell line and higher to 320% (0.32 fold increase) for the metastatic MBA-MD-231 cell line with a lower significant *p* value < 0.0001 for their difference. 1G: Linear regression analysis confirmed that tissue level of HDAC8 expression inversely increased (r^2 = 0.3952, *p* value = 0.037) by decreasing of miR-216b-5p expression.

Table 4
Correlation of miR-216b-5p and HDAC8 with clinical characteristics of the studied subjects.

		Tumor size	Grade	Lymph node invasion	Vascular invasion	Necrosis
miR-216b-5p	Spearman's ρ correlation coefficient	-0.382	-0.287	-0.373	0.057	-0.289
	p value	0.041	0.112	0.039	0.777	0.136
HDAC8	Spearman's ρ correlation coefficient	-.069	-0.051	-0.143	-0.067	-0.099
	p value	0.722	0.783	0.443	0.741	0.615

HDAC8 = Histone deacetylase 8; miR-216b-5p = microRNA-216b-5p.

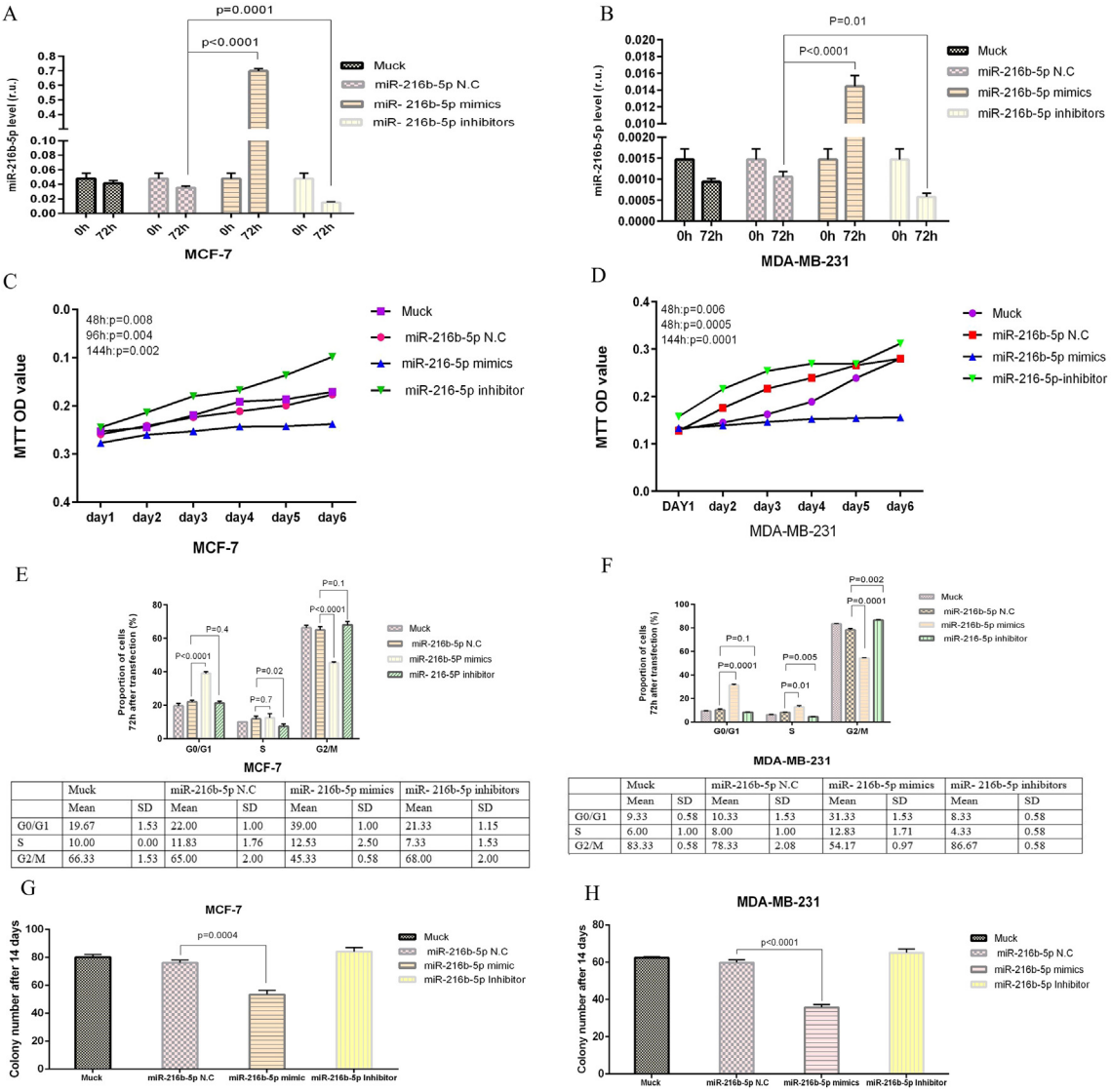

	Muck		miR-216b-5p N.C		miR- 216b-5p mimics		miR- 216b-5p inhibitors	
	Mean	SD	Mean	SD	Mean	SD	Mean	SD
G0/G1	19.67	1.53	22.00	1.00	39.00	1.00	21.33	1.15
S	10.00	0.00	11.83	1.76	12.53	2.50	7.33	1.53
G2/M	66.33	1.53	65.00	2.00	45.33	0.58	68.00	2.00

	Muck		miR-216b-5p N.C		miR- 216b-5p mimics		miR- 216b-5p inhibitors	
	Mean	SD	Mean	SD	Mean	SD	Mean	SD
G0/G1	9.33	0.58	10.33	1.53	31.33	1.53	8.33	0.58
S	6.00	1.00	8.00	1.00	12.83	1.71	4.33	0.58
G2/M	83.33	0.58	78.33	2.08	54.17	0.97	86.67	0.58

Fig. 2. Overexpression of miR-216b-5p inhibited cell proliferation and colony formation and induced G0/G1 arrest in BC cell lines. 2A and B: The relative level of miR-216b-5p after transfection with mimics inhibitor in MCF-7 (2A) and MDA-MB-231(2B) cell lines. 2C and D: MTT assay for 6 days of and MDA-MB-231 (2D) cells transfected with miR-216b-5p mimics (p value = 0.002) for MCF-7 (2C) and (p value = 0.0001) for MDA-MB-231 as compared to NC. 2E and F: BC cell lines transfection with miR-216b-5p inhibited the entry of MCF-7 (2E) and MDA-MB-231 (2F) cells into G2/M phase. 2G and H: Representative images of the colony formation assay show that, following treatment with miR-216b-5p, MCF-7 (2G) and MDA-MB-231 (2H) cells formed fewer colonies compared with controls. The number of clones formed by the MCF-7 (2G) and MDA-MB-231 (2H) cell lines were derived from the colony formation assay. Results are presented as the mean ± standard deviation from three independent experiments. p value = 0.0004 and < 0.0001 for MCF-7 and MDA-MB-231 compared with the NC.

and inhibitor, then the following overexpression or inhibition of miR-216b-5p by mimics or inhibitor were detected by qRT-PCR. As shown in Fig. 2A and B, after transfection of BC cell lines with miR-216b-5p mimics expression of miR-216b-5p significantly increased (p value < 0.0001) compared with NC and mock controls, while transfection with inhibitor down-regulated miR-216b-5p expression (p value < 0.0001 and = 0.01 for MCF-7 and MDA-MB-231, respectively). We used the MTT assay for evaluating the proliferation status of BC cell lines after transfection with miR-216b-5p mimics and inhibitors. As can be seen in Fig. 2C and D the miR-216b-5p mimics significantly inhibited proliferation of MCF-7 and MDA-MB-231 cell lines by 11% and 21% (p value = 0.008 and 0.006, respectively), 16% and 36% (p value = 0.004 and 0.0005, respectively) and 27% and 43% (p value = 0.002 and 0.0001, respectively) at 48, 96 and 144 h, respectively, as compared to the controls. On the other hand, miR-216b-5p inhibitor transfection in MCF-7 and MDA-MB-231 cell lines enhanced cell proliferation (Fig. 2C and D). We then studied the growth of the cells using a flow cytometric assay of the cell distribution. Fig. 2E and F shows the function of miR-216b-5p on cell cycle profile of MCF-7 and MDA-MB-231 cell lines at 72 h. Accordingly, overexpression of miR-216b-5p resulted in G0/G1 phase arrest in MCF-7 and MDA-MB-231 cell lines after 72 h of exposure compared with NC and mock controls, while cells treated with miR-216b-5p inhibitors showed a significant decrease in G0/G1 arrest as compared to controls (Fig. 2E and F). Finally, we further inspected the effects of miR-216b-5p on BC cells clonogenicity by a colony formation assay. Our results clearly showed that the miR-216b-5p-transfected MDA-MB-231 and MCF-7 cells formed smaller amounts of colonies per well. A significant reduction in colony formation was detected in MCF-7 and MDA-MB-231 cells transfected with miR-216b-5p mimic (Fig. 2G and H) while miR-216b-5p inhibitor transfection suppressed this effect (p Value < 0.0001).

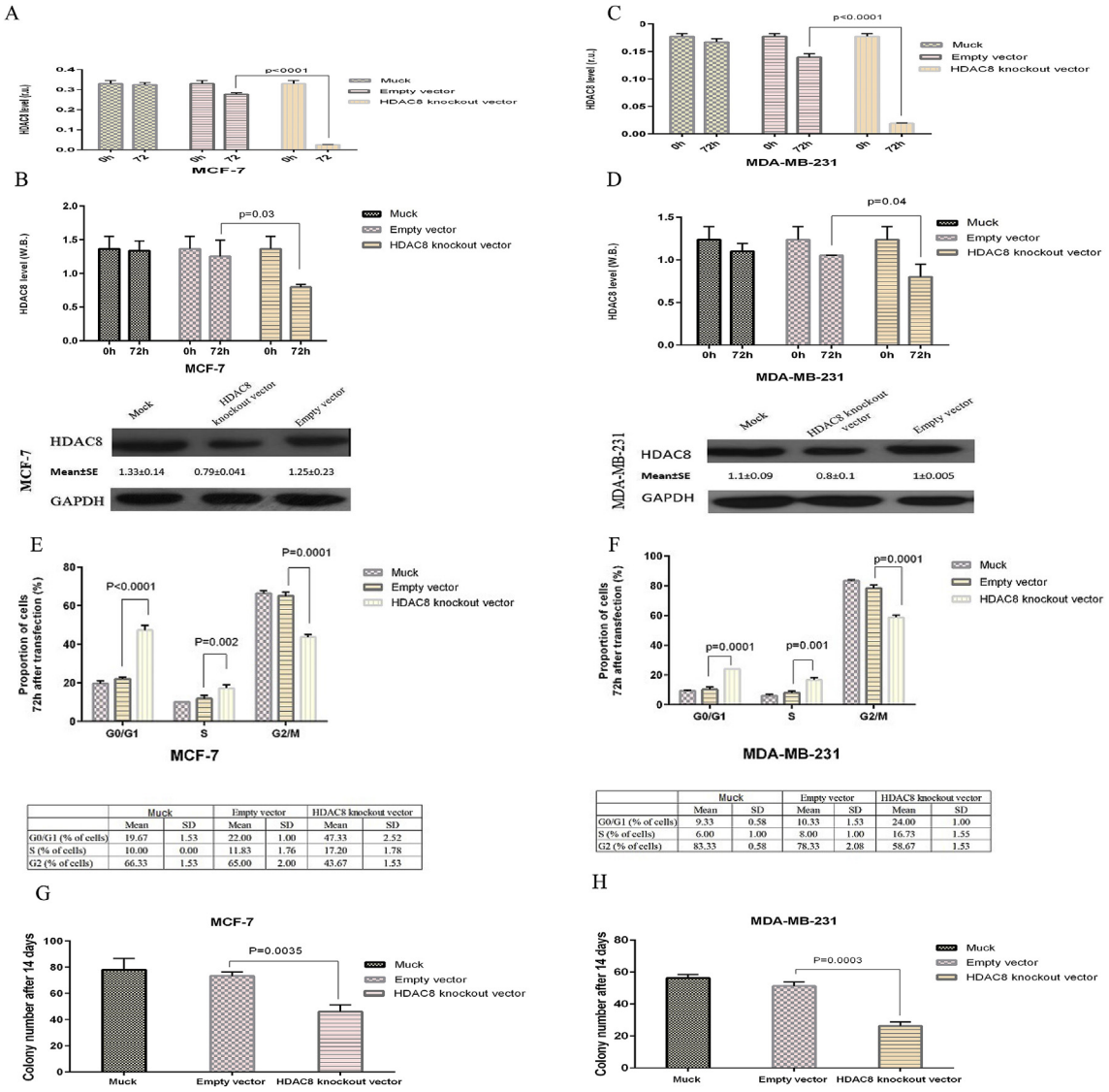

	Muck		Empty vector		HDAC8 knockout vector	
	Mean	SD	Mean	SD	Mean	SD
G0/G1 (% of cells)	19.67	1.53	22.00	1.00	47.33	2.52
S (% of cells)	10.00	0.00	11.83	1.76	17.20	1.78
G2 (% of cells)	66.33	1.53	65.00	2.00	43.67	1.53

	Muck		Empty vector		HDAC8 knockout vector	
	Mean	SD	Mean	SD	Mean	SD
G0/G1 (% of cells)	9.33	0.58	10.33	1.53	24.00	1.00
S (% of cells)	6.00	1.00	8.00	1.00	16.73	1.55
G2 (% of cells)	83.33	0.58	78.33	2.08	58.67	1.53

Fig. 3. Down-regulation of HDAC8 inhibited cell proliferation and colony formation and induced G0/G1 arrest in BC cell lines. 3A and B: The relative expression of HDAC8 extremly decreased in gene (3A) and protein (3B) level after transfection with HDAC8 knockout vector in MCF-7 cell line. 3C and D: Transfection of MDA-MB-231 cell line with HDAC8 knockout vector also resulted in highly decline in HDAC8 expression in gene (3C) and protein (3D) level. 3E and F: BC cell lines transfection with HDAC8 knockout vector inhibited the entry of MCF-7 (3E) and MDA-MB-231 (3F) cells into G2/M phase. 3G and H: Representative images of the colony formation assay show that, following treatment with HDAC8 knockout vector, MCF-7 (3G) and MDA-MB-231 (3H) cells formed fewer colonies compared with controls. The number of clones formed by the MCF-7 (3G) and MDA-MB-231 (3H) cell lines were derived from the colony formation assay. Results are presented as the mean ± standard deviation from three independent experiments. p value = 0.0035 and 0.0003 for MCF-7 and MDA-MB-231 compared with the NC.

3.3. HDAC8 is involved in miR-216b-5p -regulated proliferation, cell cycle arrest and colony formation inhibition in breast cancer cells

To identify whether HDAC8 involves in miR-216b-5p-suppressed breast cancer progression, HDAC8 was knocked out by CRISPR/Cas9 method in MDA-MB-231 and MCF-7 cell lines and BC cellular functions including proliferation, cell cycle and colony formation were checked on the knocked out selected population of the cell lines. Decline in HDAC8 expression after transfection with knockout vector were detected in RNA and protein levels using qRT-PCR and Western blot methods, respectively. qRT-PCR analysis of HDAC8 expression showed significant decrease in HDAC8 expression levels after transfection of BC cell lines with HDAC8 knockout vector compared to empty vector and mock controls (0.096 ± 0.005 and 0.14 ± 0.004 (r.u.), respectively) (Fig. 3A and C). Besides, the corresponding protein levels also confirmed the highly decline in HDAC8 in knockout group as compared to controls (0.76 ± 0.03 and 0.63 ± 0.04, respectively) (Fig. 3B and D). As shown in Fig. 3C and D, in MDA-MB-231 loss of function of the HDAC8 in gene and protein levels had higher significance value than MCF-7 cell lines. After transfection of MDA-MB-231 cell lines with HDAC8 knock out vector, the expression of HDAC8 in gene and protein level were extremely down-regulated (0.019 ± 0.0005 (r.u.), 0.8 ± 0.14, respectively) when compared to empty vector group (0.14 ± 0.006 (r.u.), 1.1 ± 0.0005, respectively) and mock group (0.17 ± 0.006 (r.u.), 1.1 ± 0.1, respectively) (p value < 0.0001, p value = 0.04). Next the capacity of cell growth was confirmed by flowcytometry and cologenicity tests. Cell cycle analysis revealed that the percentage of cells at G1/G0 phase dramatically increased from 21% to 50% and 10%–24% in MCF-7 and MDA-MB-231 cell lines after transfection with HDAC8 KO vector at 72 h after transfection (Fig. 3E and F) compared to empty vector. In addition, we used colony formation assay to investigate the role of HDAC8 on clonogenic survival, and results demonstrated that knocking out of HDAC8 caused a decrease in the clonogenic survival of MCF-7 and MDA-MB-231 cells (46 ± 5 and

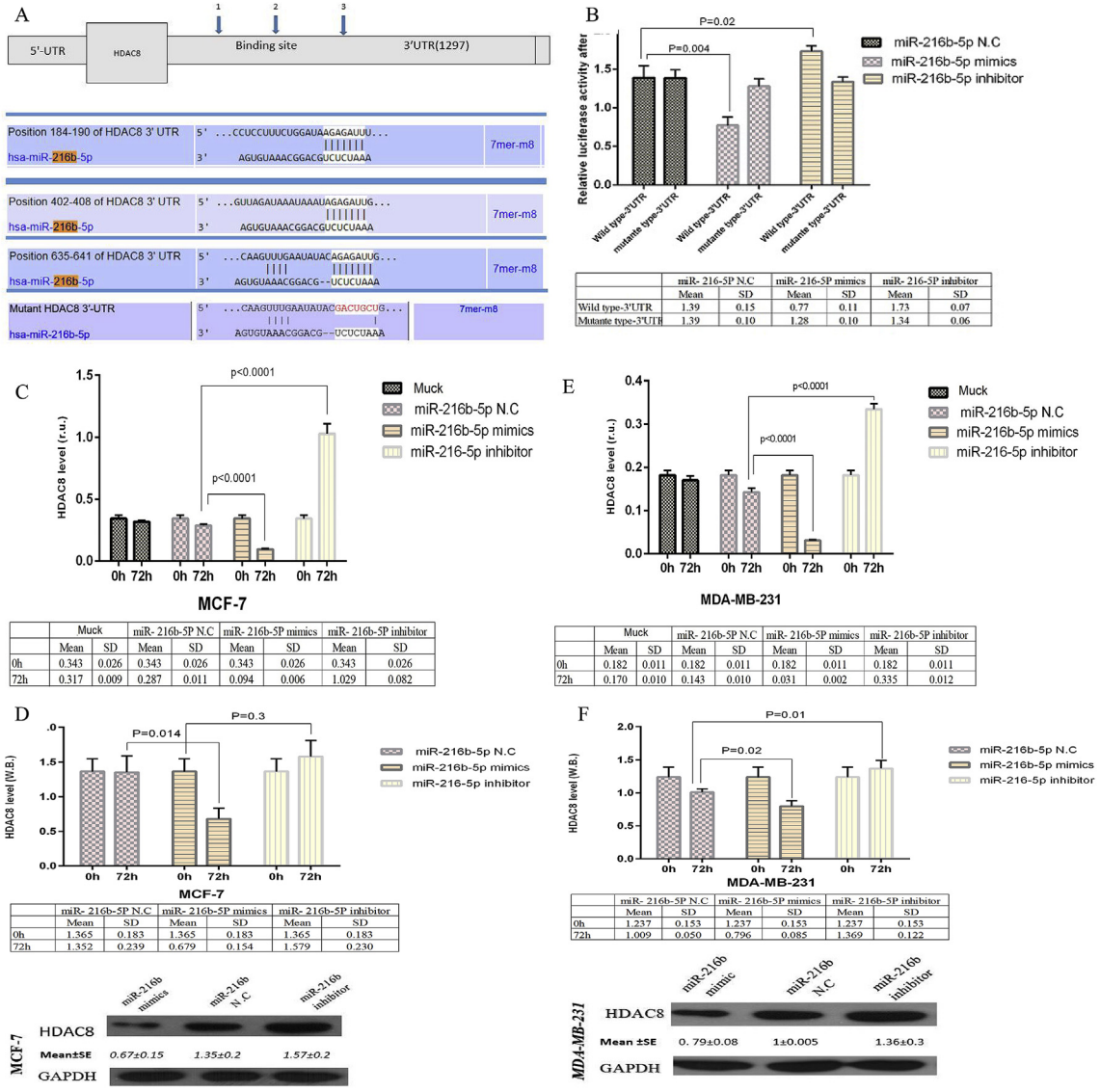

	miR- 216-5P N.C		miR- 216-5P mimics		miR- 216-5P inhibitor	
	Mean	SD	Mean	SD	Mean	SD
Wild type-3'UTR	1.39	0.15	0.77	0.11	1.73	0.07
Mutante type-3'UTR	1.39	0.10	1.28	0.10	1.34	0.06

	Muck		miR- 216b-5P N.C		miR- 216b-5P mimics		miR- 216b-5P inhibitor	
	Mean	SD	Mean	SD	Mean	SD	Mean	SD
0h	0.343	0.026	0.343	0.026	0.343	0.026	0.343	0.026
72h	0.317	0.009	0.287	0.011	0.094	0.006	1.029	0.082

	Muck		miR- 216b-5P N.C		miR- 216b-5P mimics		miR- 216b-5P inhibitor	
	Mean	SD	Mean	SD	Mean	SD	Mean	SD
0h	0.182	0.011	0.182	0.011	0.182	0.011	0.182	0.011
72h	0.170	0.010	0.143	0.010	0.031	0.002	0.335	0.012

	miR- 216b-5P N.C		miR- 216b-5P mimics		miR- 216b-5P inhibitor	
	Mean	SD	Mean	SD	Mean	SD
0h	1.365	0.183	1.365	0.183	1.365	0.183
72h	1.352	0.239	0.679	0.154	1.579	0.230

	miR- 216b-5P N.C		miR- 216b-5P mimics		miR- 216b-5P inhibitor	
	Mean	SD	Mean	SD	Mean	SD
0h	1.237	0.153	1.237	0.153	1.237	0.153
72h	1.009	0.050	0.796	0.085	1.369	0.122

Fig. 4. miR-216b-5p directly targets the 3′-UTR of HDAC8 gene. 4A: *In-silico* predicted of the pairing of miR-216b-5p to sites in the 3′-UTR of the human HDAC8 gene. 4B: Relative luciferase activity of the HDAC8 wild type 3′-UTR and mutant type 3′-UTR luciferase constructs in HEK293T cell line transfected with miR-216b-5p mimics, inhibitor or NC. 4C and D: The relative expression of HDAC8 extremly decreased in gene (4C) and protein (4D) level after transfection with miR-216b-5p mimics in MCF-7 cell line. 4E and F: Transfection of MDA-MB 231 cell line with miR-216b-5p mimics also resulted in highly decline in HDAC8 expression in gene (4E) and protein (4F) level.

26 ± 2.5 colonies, respectively) compared with empty vector (73 ± 3 and 51 ± 2 colonies, respectively) and mock group (78 ± 9 and 56 ± 2.1 colonies, respectively) (p value = 0.0035 and 0.0003, respectively). (Fig. 3G and H).

3.4. MiR-216b-5p directly targets 3′-UTR of HDAC8 mRNA

In order to search for the effective functional target of miR-216b-5p and its mechanism we used online computational miRNA target prediction algorithm (TargetScan 6.0). This algorithm predicted the 3′-UTRs of HDAC8 mRNA contain putative miR-216b-5p binding sites. We evaluated three different predicted miR- 216b-5P binding sites that were found in 3′-UTR region of HDAC8 gene (Fig. 4A). We then investigated the mechanism by which miR-216b-5p suppresses the progression of breast cancer tumors. To confirm whether HDAC8 is a direct target of miR-216b-5p, we inserted the wild-type and the 550bp-mutant form of HDAC8 3′-UTR into the psiCHECK-2 vector at the downstream of the Renilla luciferase coding sequence separately. As illustrated in Fig. 4B miR-216b-5p rather than control significantly suppressed the Renilla luciferase activity in HEK293T cells, which was compromised when the binding site of miR-216b-5p was mutated. Furthermore, we found that overexpression of miR-216b-5p reduced the endogenous HDAC8 mRNA and protein expression in both MCF-7 and MDA-MB-231 cells, whereas transfection with miR-216b-5p inhibitor increased the level of HDAC8 mRNA and protein in MCF-7 and MDA-MB-231 cells. The results were confirmed by Western blot analysis (Fig. 4C–F).

4. Discussion

In the present study, we evaluated the impact of HDAC8 and miR-216b-5p in breast cancer progression. Here, we showed that miR-216b-5p is significantly down-regulated in human breast cancer tissue and BC cell lines. We also observed that miR-216b-5p has a negative correlation with the HDAC8 level. Our results demonstrated that miR-216b-5p down regulates the expression of HDAC8 by directly targeting of the HDAC8 3′-UTR. We proved that upon miR-216b-5p overexpression, HDAC8 is significantly decreased.

Resistance to treatment with chemotherapeutic drugs and invasion and migration of BC cells are the main causes of BC-related death [14]. In addition to genetic changes, epigenetic abnormalities also play a major role in beginning and development of cancer [19]. The epigenetic mechanisms involved in cancer pathogenesis are DNA methylation, histone modification, nucleosome positioning, and noncoding RNA expression, specifically microRNA expression [19]. Studies have revealed a direct correlation between alterations in histone proteins and breast tumorigenesis [20–22]. Previous studies showed that HDAC8 is highly over expressed in triple-negative breast cancer [23] and up-regulation of HDAC8 is responsible for late stage particularly in triple-negative breast cancer and poor prognosis and poor treatment response in breast cancer [23]. Consequently, tumor development can be prevented by inhibiting this protein as a potential therapeutic target. Recently, it has been more attention to targeted inhibition of HDAC8 as a potential cancer cells growth suppressor in vitro and in vivo [24].

In line with previous studies, the current findings showed an over-expression of HDAC8 in clinical BC specimens and breast cancer cell lines. We confirmed the oncogenicity of HDAC8 in breast cancer through a loss of function experiment. We found that oncogenic function of HDAC8 is significantly decreasedfollowing transfection the BC cell lines with HDAC8-KO-vector.

Altered expressions of different miRNAs have been also reported as factors affecting in pathogenesis of breast cancer [25,26]. Previous studies revealed the anti-tumor role of miR-216 in nasopharyngeal carcinoma [12], colorectal cancer [27], breast cancer [15] and hepatocellular carcinoma [13]. miR-216 is also proposed as a potential regulator of the apoptosis by interacting with c-Jun [28] and Autophagy [29]. Different cancer studies introduced various potential targets for miR-216b-5p, although all studies have emphasized on the anti-tumor properties of miR-216b-5p; for instance UDP-glucuronosyltransferase (UGT) 2B in liver cancer cell line [30], translationally controlled tumor protein (TPT1) in Pancreatic Cancer Cells [31], and Pyridoxine 5′-phosphate oxidase (PNPO) in human breast invasive ductal carcinoma development [32]. However the role of miR-216b-5p for the regulation of HDAC8 has not been studied yet. Our result, for the first time, explain that the miR-216b-5p function as a tumor suppressor and inhibit the proliferation, cell growth and colony formation by regulating the expression of HDAC8 in breast cancer.

More interestingly, changes in *HDAC8* and *miR-216b-5p* followed a similar pattern in both metastatic triple negative basal like (MDA-MB-231) and non metastatic luminal A (MCF-7) cell lines. Due to various histopatologic properties of the breast cancer subtypes, Molecular mechanisms involved in disease development and progression are very diverse [33]. Accordingly, despite the similar alterations pattern, we observed that over-expression *miR-216b-5p* or suppression of *HDAC8* created more cytotoxic effects in MDA-MB-231 cell line compared to MCF-7 cell lines.

The β-catenin/Wnt signaling pathway is an important molecular mechanism which initiates the epithelial–mesenchymal transition (EMT) process [34–36]. This mechanism is also involves in breast cancer tumorigenesis and metastasis [37], thereby, EMT targeted-therapy creats a promising future in breast cancer treatment. In addition, it has been previously showed that *HDAC8* potentially activates the Wnt/β-catenin signaling pathway [38]. A proposed mechanism for tumor suppressor effects of microRNAs may relate to targeting the genes that influence the EMT process such as HDAC8 [7]. The anti-tumor property of miR-216b-5p is likely to be applied in this manner.

In conclusion, our results revealed the anti-tumor role of miR-216b-5p on HDAC8 resulting to inhibition of breast cancer proliferation and progression. Our data showed that inhibition of HDAC8 via miR-261-5p maybe proposed as a potential therapeutic approach for future studies.

Ethical approval

All procedures performed in studies involving human participants were in accordance with the ethical standards of the ethics committee of Kurdistan University of Medical Sciences and with the 1964 Helsinki declaration and its later amendments or comparable ethical standards.

Informed consent

Informed consent was obtained from all individual participants included in the study.

Funding source

This work was supported by a research grant from Kurdistan University of Medical Sciences, Sanandaj, Iran (Grant/Award Number: ‘IR.MUK.REC.1395/279’).

Financial disclosure

The author has no financial relationships relevant to this article to disclose.

Author contributions

M-N.M. and N.D. carried out the experiment. K.R. helped supervise the project. A.A., S.M-Y., and V.H. conceived and planned the experiments. A.E. provided the BC samples. M.A. took the lead in project, conceived the original idea, supervised the project, analyzed the results and wrote the manuscript with support from K.R. and S.M-Y.

Declaration of Competing interest

Dr MN Menbari declares no potential conflicts of interest with respect to the research, authorship, and/or publication of this article. Dr K Rahimi declares that he has no conflict of interest. Dr A Ahmadi declares that he has no conflict of interest. Dr A Elyasi declares that he has no conflict of interest. Dr. N Darvishi declares that she has no conflict of interest. Dr V hosseini declares that she has no conflict of interest. Dr S Mohammadi-Yeganeh declares that she has no conflict of interest. Dr M Abdi has received research grants from Kurdistan University of medical sciences.

Acknowledgments

The author wish to thank all patients and health stuffs who participated in this study. Financial support from Kurdistan University of medical sciences is highly appreciated.

References

[1] R.L. Siegel, K.D. Miller, A. Jemal, Cancer statistics, 2018. CA Cancer J Clin 68 (1) (2018 Jan) 7–30.
[2] E. Gourd, Low uptake of tamoxifen to prevent breast cancer, Lancet Oncol. (2018 May 3) S1470-2045(18)30344-9.
[3] H. Zhang, Y.P. Shang, H.Y. Chen, J. Li, Histone deacetylases function as novel potential therapeutic targets for cancer, Hepatol. Res. 47 (2) (2017 Feb) 149–159.
[4] A. Chakrabarti, I. Oehme, O. Witt, G. Oliveira, W. Sippl, C. Romier, et al., HDAC8: a multifaceted target for therapeutic interventions, Trends Pharmacol. Sci. 36 (7) (2015 Jul) 481–492.
[5] M. Huang, M. Geng, Exploiting histone deacetylases for cancer therapy: from hematological malignancies to solid tumors, Sci. China Life Sci. 60 (1) (2017 Jan) 94–97.
[6] P. An, J. Li, L. Lu, Y. Wu, Y. Ling, J. Du, et al., Histone deacetylase 8 triggers the migration of triple negative breast cancer cells via regulation of YAP signals, Eur. J. Pharmacol. 845 (2019 Feb 15) 16–23.
[7] M.N. Menbari, K. Rahimi, A. Ahmadi, S. Mohammadi-Yeganeh, A. Elyasi, N. Darvishi, et al., miR-483-3p suppresses the proliferation and progression of human triple negative breast cancer cells by targeting the HDAC8 oncogene, J. Cell. Physiol. (2019 Sep 11) 10.1002/jcp.29167. [Epub ahead of print].
[8] I. Oehme, H.E. Deubzer, D. Wegener, D. Pickert, J.P. Linke, B. Hero, et al., Histone deacetylase 8 in neuroblastoma tumorigenesis, Clin. Cancer Res. 15 (1) (2009 Jan 1) 91–99.
[9] M.A. Moser, A. Hagelkruys, C. Seiser, Transcription and beyond: the role of

mammalian class I lysine deacetylases, Chromosoma 123 (1–2) (2014 Mar) 67–78.
[10] A.M. Mohr, J.L. Mott, Overview of microRNA biology, Semin. Liver Dis. 35 (1) (2015 Feb) 3–11.
[11] M. Acunzo, G. Romano, D. Wernicke, C.M. Croce, MicroRNA and cancer–a brief overview, Adv Biol Regul 57 (2015 Jan) 1–9.
[12] M. Deng, H. Tang, Y. Zhou, M. Zhou, W. Xiong, Y. Zheng, et al., miR-216b suppresses tumor growth and invasion by targeting KRAS in nasopharyngeal carcinoma, J. Cell Sci. 124 (Pt 17) (2011 Sep 1) 2997–3005.
[13] F.Y. Liu, S.J. Zhou, Y.L. Deng, Z.Y. Zhang, E.L. Zhang, Z.B. Wu, et al., MiR-216b is involved in pathogenesis and progression of hepatocellular carcinoma through HBx-miR-216b-IGF2BP2 signaling pathway, Cell Death Dis. 6 (2015 Mar 5) e1670.
[14] S. Jana, S. Sengupta, S. Biswas, A. Chatterjee, H. Roy, A. Bhattacharyya, miR-216b suppresses breast cancer growth and metastasis by targeting SDCBP, Biochem. Biophys. Res. Commun. 482 (1) (2017 Jan 1) 126–133.
[15] L. Zheng, X. Zhang, F. Yang, J. Zhu, P. Zhou, F. Yu, et al., Regulation of the P2X7R by microRNA-216b in human breast cancer, Biochem. Biophys. Res. Commun. 452 (1) (2014 Sep 12) 197–204.
[16] S. Edge, D. Byrd, C. Compton, AJCC (American Joint Committee on Cancer). Cancer Staging Manual, 7th Edition, Springer-Verlag, New York, 2010.
[17] C.W. Elston, Classification and grading of invasive breast carcinoma, Verh. Dtsch. Ges. Pathol. 89 (2005) 35–44.
[18] C. Hojland Knudsen, E.S. Asgrimsdottir, K. Rahimi, K.P. Gill, S. Frandsen, S. Hvolbol Buchholdt, et al., A modified monomeric red fluorescent protein reporter for assessing CRISPR activity, Front Cell Dev Biol 6 (2018) 54.
[19] H. Shen, L. Li, S. Yang, D. Wang, S. Zhong, J. Zhao, et al., MicroRNA-29a contributes to drug-resistance of breast cancer cells to adriamycin through PTEN/AKT/GSK3beta signaling pathway, Gene 593 (1) (2016 Nov 15) 84–90.
[20] R. Kanwal, K. Gupta, S. Gupta, Cancer epigenetics: an introduction, Methods Mol. Biol. 1238 (2015) 3–25.
[21] R. Connolly, V. Stearns, Epigenetics as a therapeutic target in breast cancer, J. Mammary Gland Biol. Neoplasia 17 (3–4) (2012 Dec) 191–204.
[22] E. Koeneke, O. Witt, I. Oehme, HDAC family members intertwined in the regulation of autophagy: a druggable vulnerability in aggressive tumor entities, Cells 4 (2) (2015 Apr 23) 135–168.
[23] C.L. Hsieh, H.P. Ma, C.M. Su, Y.J. Chang, W.Y. Hung, Y.S. Ho, et al., Alterations in histone deacetylase 8 lead to cell migration and poor prognosis in breast cancer, Life Sci. 151 (2016 Apr 15) 7–14.
[24] I. Rettig, E. Koeneke, F. Trippel, W.C. Mueller, J. Burhenne, A. Kopp-Schneider, et al., Selective inhibition of HDAC8 decreases neuroblastoma growth in vitro and in vivo and enhances retinoic acid-mediated differentiation, Cell Death Dis. 6 (2015 Feb 19) e1657.
[25] A. Bischoff, B. Huck, B. Keller, M. Strotbek, S. Schmid, M. Boerries, et al., miR149 functions as a tumor suppressor by controlling breast epithelial cell migration and invasion, Cancer Res. 74 (18) (2014 Sep 15) 5256–5265.
[26] Z. Liang, X. Bian, H. Shim, Inhibition of breast cancer metastasis with microRNA-302a by downregulation of CXCR4 expression, Breast Canc. Res. Treat. 146 (3) (2014 Aug) 535–542.
[27] S.Y. Kim, Y.H. Lee, Y.S. Bae, MiR-186, miR-216b, miR-337-3p, and miR-760 cooperatively induce cellular senescence by targeting alpha subunit of protein kinase CKII in human colorectal cancer cells, Biochem. Biophys. Res. Commun. 429 (3–4) (2012 Dec 14) 173–179.
[28] Z. Xu, Y. Bu, N. Chitnis, C. Koumenis, S.Y. Fuchs, J.A. Diehl, miR-216b regulation of c-Jun mediates GADD153/CHOP-dependent apoptosis, Nat. Commun. 7 (2016 May 13) 11422.
[29] Z. Chen, S. Gao, D. Wang, D. Song, Y. Feng, Colorectal cancer cells are resistant to anti-EGFR monoclonal antibody through adapted autophagy, Am J Transl Res 8 (2) (2016) 1190–1196.
[30] D.F. Dluzen, A.K. Sutliff, G. Chen, C.J. Watson, F.T. Ishmael, P. Lazarus, Regulation of UGT2B expression and activity by mir-216b-5p in liver cancer cell lines, J. Pharmacol. Exp. Ther. 359 (1) (2016 Oct) 182–193.
[31] Y. You, J. Tan, Y. Gong, H. Dai, H. Chen, X. Xu, et al., MicroRNA-216b-5p functions as a tumor-suppressive RNA by targeting TPT1 in pancreatic cancer cells, J. Cancer 8 (14) (2017) 2854–2865.
[32] W. Ren, W. Guan, J. Zhang, F. Wang, G. Xu, Pyridoxine 5'-phosphate oxidase is correlated with human breast invasive ductal carcinoma development, Aging (Albany NY) 11 (7) (2019 Apr 14) 2151–2176.
[33] G.K. Malhotra, X. Zhao, Band H, Band V. Histological, molecular and functional subtypes of breast cancers, Cancer Biol. Ther. 10 (10) (2010 Nov 15) 955–960.
[34] R. Kalluri, R.A. Weinberg, The basics of epithelial-mesenchymal transition, J. Clin. Investig. 119 (6) (2009 Jun) 1420–1428.
[35] J.P. Thiery, H. Acloque, R.Y. Huang, M.A. Nieto, Epithelial-mesenchymal transitions in development and disease, Cell 139 (5) (2009 Nov 25) 871–890.
[36] E. Vincan, N. Barker, The upstream components of the Wnt signalling pathway in the dynamic EMT and MET associated with colorectal cancer progression, Clin. Exp. Metastasis 25 (6) (2008) 657–663.
[37] G.B. Jang, J.Y. Kim, S.D. Cho, K.S. Park, J.Y. Jung, H.Y. Lee, et al., Blockade of Wnt/beta-catenin signaling suppresses breast cancer metastasis by inhibiting CSC-like phenotype, Sci. Rep. 5 (2015 Jul 23) 12465.
[38] Y. Tian, V.W. Wong, G.L. Wong, W. Yang, H. Sun, J. Shen, et al., Histone deacetylase HDAC8 promotes Insulin resistance and beta-catenin activation in NAFLD-associated hepatocellular carcinoma, Cancer Res. 75 (22) (2015 Nov 15) 4803–4816.